Kinetics and Transport Effects in the Dehydration of Crystalline Potassium Carbonate Hydrate

M. A. STANISH and
D. D. PERLMUTTER

Department of Chemical Engineering
University of Pennsylvania
Philadelphia, PA 19104

The reaction kinetics and physical transport processes governing the thermal dehydration of solid $K_2CO_3 \cdot 3/2H_2O$ particles were investigated. Isothermal reaction rate data were gathered using a thermogravimetric balance in which narrowly-sized $K_2CO_3 \cdot 3/2H_2O$ crystals were dehydrated under a water vapor atmosphere at different pressures and temperatures. The magnitudes of the heat and mass transfer resistances external to and within the solid product were estimated from solutions of the relevant pseudosteady-state transport equations. In the temperature range 320 to 358 K, the vacuum dehydration of $K_2CO_3 \cdot 3/2H_2O$ crystals smaller than 710 μm (−25 +30 mesh) are accurately modeled by the spherical shrinking-core equation for the chemical rate control regime. In the presence of water vapor, external heat transfer to the particles was sufficient to prevent significant self-cooling; heat and mass transfer resistances within the particles were negligible. The activation energy for $K_2CO_3 \cdot 3/2H_2O$ dehydration is approximately 91 kJ/mol in vacuum; the reaction becomes extremely slow at relative pressures $(P/P_{eq}) > 0.35$.

SCOPE

Of the literature reports concerned with the dehydration of solid inorganic salt hydrates, a majority are based on information from experiments done in vacuum or in dry atmospheres; as a consequence, the dehydration reaction is most often treated as an irreversible thermal decomposition. The possible application of salt hydrates as absorbents in chemical heat pumps (Stanish and Perlmutter, 1981) provides an incentive to investigate the dehydration of these materials in greater detail and suggests that this process should be treated instead as one part of a reversible gas-solid reaction.

This paper reports the results of experimental rate studies of the dehydration of $K_2CO_3 \cdot 3/2H_2O$, a salt hydrate that holds promise as a heat pump absorbent. Experimentally-measured particle reaction data are interpreted in terms of a shrinking-core gas-solid reaction model. The dehydration rate dependence on ambient water vapor pressure is of primary interest and is quantitatively determined for temperature in the range 338 to 358 K. Internal and external heat and mass transfer resistances are estimated for the conditions employed and their roles in the overall particle hydration process are evaluated.

CONCLUSIONS AND SIGNIFICANCE

The dehydration of small crystals of $K_2CO_3 \cdot 3/2H_2O$ may be accurately modeled by the spherical shrinking-core equation for the chemical rate control regime. In the presence of water vapor, heat transfer rates to the particles are sufficiently high to prevent significant self-cooling. Under vacuum conditions, self-cooling becomes important; particle temperature corrections were calculated from a heat balance equation that takes account of the radiation heat transfer to the solid particles and supporting sample pan. In either atmosphere, heat transfer resistance within the particle is negligible. Diffusional resistances within the product layer are not important for particles smaller than about 710 μm (−25 +30 mesh), but are likely to become significant in particles only several times greater in diameter.

The activation energy for $K_2CO_3 \cdot 3/2H_2O$ dehydration is approximately 91 kJ/mol. Measured as the velocity of travel of the reaction interface, the dehydration rate is strongly inhibited by the presence of water vapor; the reaction becomes extremely slow at relative pressures greater than $P/P_{eq} \cong 0.35$.

INTRODUCTION

This paper reports experimental and interpretative results of a study of the dehydration of an inorganic salt hydrate. Aside from its inherent interest as an example of solid-decomposition kinetics, this investigation was motivated by a recent report (Stanish and Perlmutter, 1981) showing that heat pump cycles employing solid salt hydrates compare favorably to previously proposed solid or liquid absorbents on the basis of thermodynamic performance efficiencies. Such systems have attracted particular attention (Baughn and Jackman, 1974), because they can provide heating, cooling and energy storage capabilities in a single unit and thus offer the possibility of significantly reduced average annual costs through year-round operation of solar-powered units. It should be noted, however, that the chemical reactions involved in the operation of a hydrate-based heat pump are not well understood, nor are kinetic data commonly available for the dehydration and rehydration of solid inorganic salts.

The bulk of early work on salt hydrate decomposition has been reviewed by Lyakhov and Boldyrev (1972). Other investigators have studied these reactions in a variety of ambient atmospheres, among which the most relevant to absorption heat pump appli-

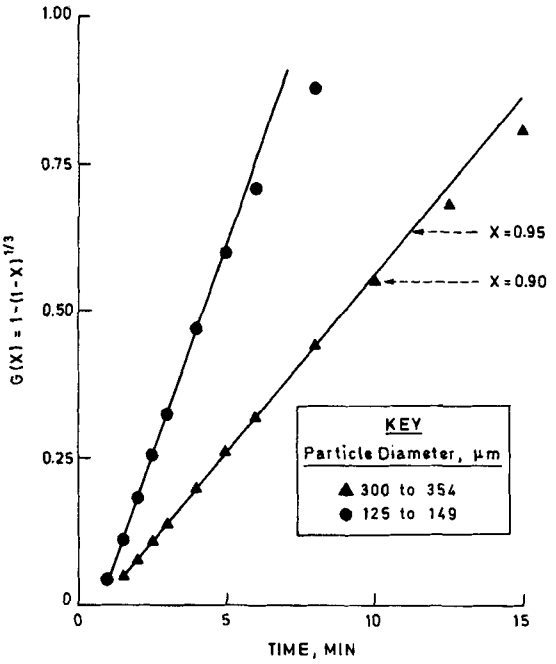

Figure 1. Vacuum dehydration data for $K_2CO_3 \cdot 3/2H_2O$ crystals at $T = 340.5$ K and the fit of the spherical shrinking core equation under chemical rate control.

cations are those that consider rate dependence on water vapor pressure (Acock et al., 1946; Anous et al., 1951; Fichte and Flanagan, 1971; Gardet et al., 1976). The effect of diffusional resistances on dehydration rate was recognized by Smith and Topley (1931), who labelled the phenomenon "impedance". Rather than quantify this factor, Smith and Topley attempted to eliminate it by extrapolating their observed rate conversion curves back to zero reaction. Cooper et al. (1933) followed the same procedure and reported that the impedance effect on $CuSO_4 \cdot 3H_2O$ dehydration increased with temperature. The magnitude of the impedance phenomenon may depend on the temperature, water vapor pressure, and on the particular hydrate considered. Smith and Topley observed, for example, that the effect of impedance on $CuSO_4 \cdot 5H_2O$ dehydration at 295.4 K all but disappeared at a pressure of 5 Pa. The authors concluded that the relative importance of diffusion is proportional to the absolute reaction rate, which falls rapidly with increasing pressure. In contrast to copper sulfate hydrates, chrome alum does not appear to exhibit the impedance effect (Cooper and Garner, 1940).

Heat transfer resistances, like the mass transfer resistance responsible for the impedance phenomenon, can also be important in dehydration reactions. External resistances may give rise to the effect known as "self-cooling," in which the temperature of the solid drops, because the heat transferred is insufficient to sustain the endothermic reaction at the thermostatted temperature. This is most likely to happen during vacuum dehydrations when the only mode of heat transfer is via radiation, relatively inefficient at the typically low experimental temperatures. Smith and Topley found that low pressures of hydrogen (27 Pa) provided sufficient external heat transfer to virtually eliminate self-cooling but that these also restricted water vapor diffusion away from the solid to a significant extent.

Cooper and Garner measured the self-cooling of chrome alum in a hard vacuum directly, and reported that the temperature remained constant for a considerable fraction of the decomposition. Anous et al. (1951) reported that the self-cooling of chrome alum at 298 K in a vacuum was nearly the same for all crystals larger than 1 g, but that it decreased rapidly with decreasing size for smaller particles. Also, the temperature during dehydration was nearly constant for the larger crystals. McAdie (1964) reported similar results for the dehydration of $CaSO_4 \cdot 2H_2O$; the solid temperature remained essentially constant at 393 K during the first stage of a dehydration carried out at 412 K and 27 kPa water vapor partial pressure.

EXPERIMENTAL PROCEDURES

Experiments were performed with J. T. Baker Chemical Co. reagent grade $K_2CO_3 \cdot 3/2H_2O$, separated by sieving into relatively narrow particle-size ranges. The dehydration behavior of samples weighing 5 to 10 mg was observed in a Dupont model 951 Thermogravimetric Analyzer (TGA) connected to a vacuum pump and to a water vapor pressure control system. Sample temperature was maintained by the TGA furnace and measured by a chromel-alumel thermocouple placed adjacent to the sample pan. The output of this thermocouple and the weight of the hydrate sample were recorded as a function of time. Pore-size distribution data were measured with a Micromeritics model 915 mercury intrusion porosimeter.

All dehydration experiments began with the evacuation of the TGA balance housing and connecting lines at room temperature followed by at least two flushes with water vapor to eliminate all other gases. No change in sample weight was observed during this pretreatment. The water vapor pressure and furnace temperature were then increased simultaneously at constant sample weight, until the temperature of interest was reached. After several minutes of equilibration, the balance housing was connected to a flask containing either distilled water or saturated $CaCl_2 \cdot 6H_2O$ solution and maintained at the saturation temperature of the water vapor pressure of interest. The pressure in the housing thus fell immediately to this preselected level, initiating the isothermal, isobaric dehydration.

RESULTS AND DISCUSSION

Dehydration Kinetics

Under an optical microscope, the $K_2CO_3 \cdot 3/2H_2O$ particles appeared irregular in shape; the larger size from 590 to 710 μm (−25 + 30 mesh) were more rounded and spherical, and the smaller sizes from 125 to 149 μm (−100 + 120 mesh) more angular and platelike. On a heated stage, nucleation of the dehydration product K_2CO_3 was observed to occur over most of the surface area of each hydrate particle. The interface between the reactant and product phases subsequently moved inward through the particle, forming a shrinking core of reactant surrounded by a product layer of increasing thickness. On the basis of these observations, several shrinking core model equations for solid decompositions (Sharp et al., 1966) were compared to the observed dehydration behavior.

The spherical shrinking core model assumes that in a reacting spherical particle of initial radius r_o, there exists an unreacted core of decreasing radius r surrounded by a growing product layer. If $\dot{r} \equiv dr/dt$ is constant, the model equation for chemical reaction rate control is

$$G(X) = 1 - (1 - X)^{1/3} = \left(\frac{-\dot{r}}{r_o}\right)t \qquad (1)$$

suggesting the linearity test of the data shown in Figure 1. The data presented are representative of the vacuum dehydration experiments performed over a range of temperatures and on two different sieve fractions of $K_2CO_3 \cdot 3/2H_2O$ crystals. The expected linearity persists to over 90% conversion, and the slope of this line, $-\dot{r}/r_o$, is the normalized velocity of the dehydration interface for the given particle size. Similar tests of the data were applied to variations of the shrinking-core model based on cylindrical particles or on product layer diffusion control, but none of these improved on the spherical shrinking-core equation with chemical reaction rate control. The interface velocities determined from slopes, Figure 1, are shown on Arrhenius coordinates in Figure 2. An activation energy of 87 ± 6 kJ/mol H_2O is obtained from the slope of the low-temperature section.

A set of dehydration experiments was also carried out at a number of different pressures of pure water vapor at three temperatures (338, 348 and 358 K) and for three different particle sizes. Each sample was exposed briefly to a vacuum at the temperature of interest before establishing a constant water vapor pressure to

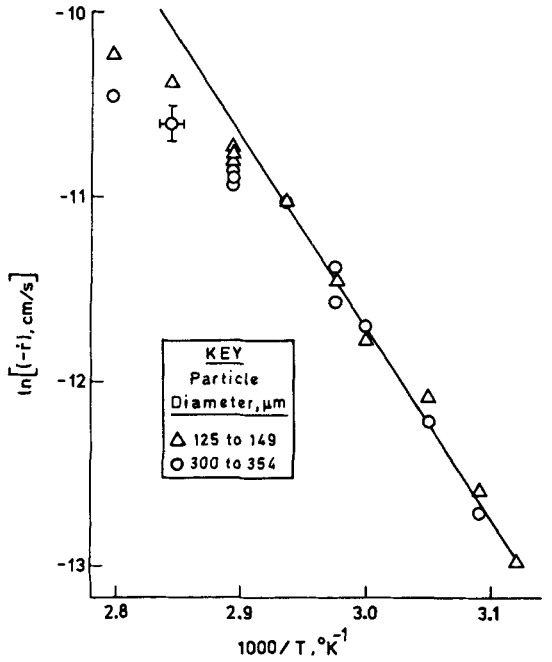

Figure 2. Vacuum dehydration rates of $K_2CO_3 \cdot 3/2H_2O$ on Arrhenius coordinates.

ensure that the dehydration had begun uniformly over the entire surface of each particle. The data were treated as in Figure 1 to determine the normalized interface velocity for each particle size at each temperature and pressure. The values of $-\dot{r}/r_o$ obtained are presented against inverse particle radius in Figures 3 and 4 both as a check on the model through the predicted inverse particle-size dependence and as a way to obtain the specific interface velocities from the slopes of the lines. The values of the velocities obtained are plotted in Figure 5 against the relative pressure, based on the vapor pressure of $K_2CO_3 \cdot 3/2H_2O$, for the three temperatures studied.

Effects of Transport Phenomena

It is well known that resistances to heat and mass transfer can play important roles in determining the rate of reaction between a gas and a solid. An abundance of theoretical gas-solid reaction models have been proposed, including pore or grain models (Szekely and Evans, 1970, 1971) and shrinking-core models under isothermal (Ishida and Wen, 1968; Wen, 1968) and nonisothermal conditions (Shen and Smith, 1965; Ishida and Shirai, 1969; Wen and Wang, 1970). The vast majority of these models were developed for irreversible chemical reactions; Ishida and Shirai (1970) and Ishida et al. (1970) are among the very few to consider the field of reversible noncatalytic gas-solid reactions to which belong the dehydration and rehydration reactions.

In addition to that of irreversible reaction, virtually all theoretical gas-solid reaction models contain an assumption of first-order chemical kinetics. In view of the results in Figure 5 showing that dehydration kinetics for $K_2CO_3 \cdot 3/2H_2O$ are more complicated than the simple first-order law, a more fundamental approach is needed in evaluating the effects of heat and mass transfer on the experiments performed in this work.

Thermal Effects

The pseudosteady-state assumption is commonly used in gas-solid reaction models. For $K_2CO_3 \cdot 3/2H_2O$, $C_p/\Delta H \cong 0.002\ K^{-1}$, implying that an adiabatic change of 1 K in the temperature of the solid would drive the reaction to a marginal conversion of only 0.002. The sensible heat released by transient cooling of any likely magnitude can, therefore, be responsible for only a very small fraction of the dehydration reaction. The pseudosteady-state approximation is thus applicable; temperature transients may be taken as very rapid and heat transport considered the only source of energy for the dehydration. For a spherical particle undergoing shrinking-core dehydration, the equation governing heat transfer through the spherical shell of product is

$$\lambda \left[\frac{1}{r^2}\frac{\partial}{\partial r}\left(r^2 \frac{\partial T}{\partial r}\right)\right] = 0 \qquad (2)$$

with the boundary condition at the surface of the unreacted core

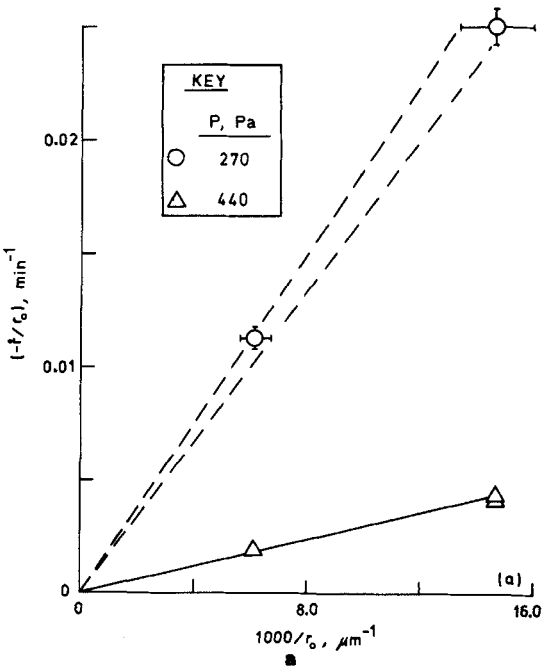

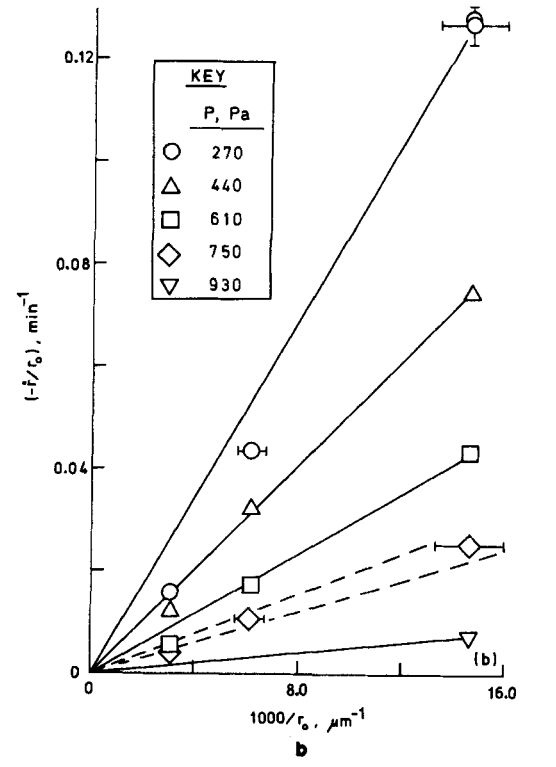

Figure 3. Dehydration rate constants derived from the spherical shrinking core model for $K_2CO_3 \cdot 3/2H_2O$ crystals at different temperatures and pressures; (a) $T = 338$ K, (b) $T = 348$ K.

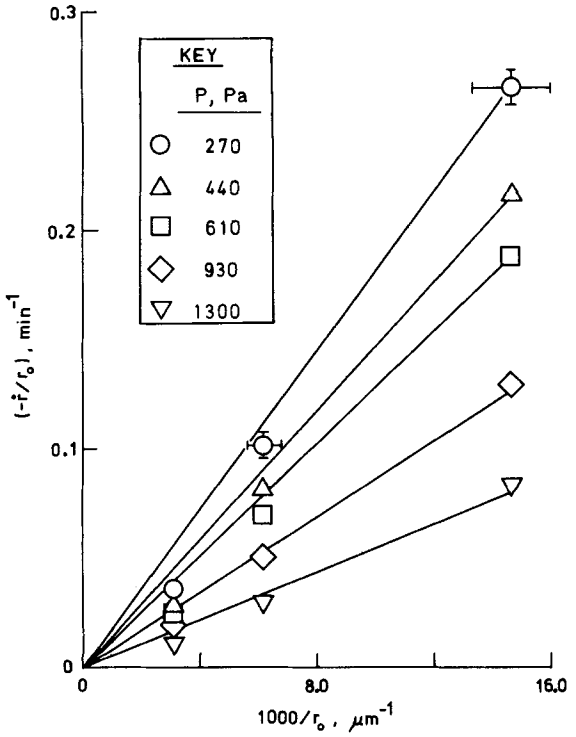

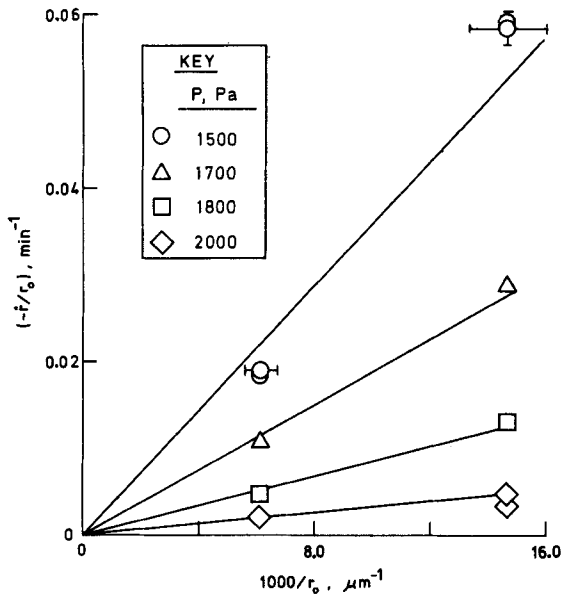

Figure 4. Dehydration rate constants derived from the spherical shrinking core model for $K_2CO_3 \cdot 3/2H_2O$ crystals at T = 358 K and different pressures.

$$\lambda \frac{\partial T}{\partial r} = \rho \, \Delta H \, (-\dot{r}), \, r = r_s \tag{3}$$

and

$$T = T_p, \, r = r_o \tag{4}$$

at the external surface of the particle. In Eq. 3, the heat flux has been set equal to the heat of reaction per unit area of interface, where λ is the thermal conductivity of the product layer, ΔH is the enthalpy of dehydration, ρ is the density of water in the hydrate crystal, and $-\dot{r}$ is the interface velocity.

The solution to Eqs. 2, 3 and 4 gives the temperature profile across the product layer as

$$T = T_p - (\Delta H \rho r_s(-\dot{r})/\lambda)(r_s/r - r_s/r_o) \tag{5}$$

from which one obtains the temperature difference between the surface of the particle and the surface of the unreacted core:

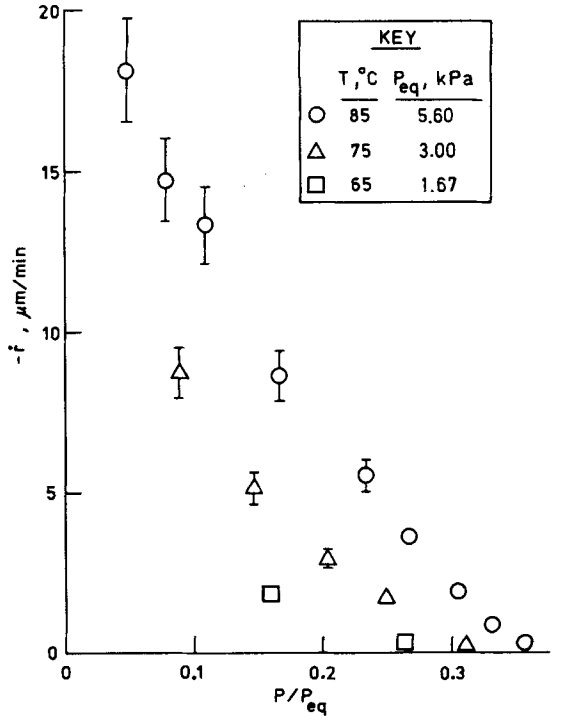

Figure 5. Rate of movement of the dehydration interface in $K_2CO_3 \cdot 3/2H_2O$ crystals as a function of reduced pressure at different temperatures.

$$(T_p - T_s) = (\Delta H \rho r_o \bar{r}(1 - \bar{r})/\lambda)(-\dot{r}) \tag{6}$$

where $\bar{r} \equiv r_s/r_o$. It may be seen from Eq. 6 that the temperature drop across the product layer is proportional to the particle size r_o and the dehydration rate $(-\dot{r})$. For $K_2CO_3 \cdot 3/2H_2O$, ΔH = 3,500 kJ/kg and ρ = 334 kg/m^3. The thermal conductivity (λ) of K_2CO_3 is not readily available in the literature; however, the conductivities of most inorganic salts are of the order of 4W/m·K, and this estimate will suffice for the purpose at hand. The largest interface velocities calculated for the dehydration experiments in this research were approximately 20 μm/min. Using this value and the 590 to 710 μm diameter of the largest particles studied (−25 + 30 mesh), an upper bound on the product layer temperature drop in any experiment was calculated from Eq. 6 with $\bar{r}$ = 0.5. The result, $T_p - T_p$ = 0.008 K, indicates that the effect is negligible. Had the thermal conductivity estimate been in error by as much as two orders of magnitude (due for example to the effect of porosity on conductivity), the estimated temperature difference would still be less than 1 degree.

The net rate of heat transfer by radiation from a furnace to a spherical particle of radius r_o is

$$Q_r = 4\pi\epsilon r_o^2 \, (5.67 \times 10^{-8})(T_b^4 - T_p^4) \tag{7}$$

where ϵ is the emissivity and T_p is the temperature at the external surface of the particle, T_b is the bulk temperature of the furnace and of the gas surrounding the particle. In a stagnant gas (Nusselt number = 2), the rate of heat transfer to the particle by conduction is

$$Q_c = 4\pi r_o \lambda_v (T_b - T_p) \tag{8}$$

where λ_v is the thermal conductivity of the vapor phase.

The temperature difference between the bulk gas and the external surface of the particle may be estimated by setting the heat required by the reaction equal to the sum of the heat transfer rates given by Eqs. 7 and 8. The result is:

$$\lambda_v(T_b - T_p) + (5.67 \times 10^{-8}) \, r_o \, \epsilon \, (T_b^4 - T_p^4) = \Delta H \rho r_o \bar{r}^2(-\dot{r}) \tag{9}$$

The temperature difference between the bulk gas and the external surface of a particle (i.e., the self-cooling) thus depends on the dehydration rate $(-\dot{r})$, degree of conversion $(\bar{r})$, and particle

Table 1. Estimated Maximum Degrees of Self-Cooling for Dehydration of $K_2CO_3 \cdot 3/2H_2O$ Particles in Water Vapor

Temp. K	Pres. Pa	Calc. Interface velocity, μm/min	Calc. self-cooling, K 590 to 710μm (−25 + 30 Mesh)	Calc. self-cooling, K 125 to 149μm (−100 +120 Mesh)
358	270	17	4.4	1.0
358	610	12.3	3.2	0.76
358	1,300	5.4	1.4	0.33
358	1,850	0.86	0.22	0.05
348	270	7.8	2.0	0.48
348	750	1.7	0.45	0.10
338	270	1.7	0.45	0.11

size (r_o) via Eq. 9. The maximum possible self-cooling (when $\bar{r}$ = 1) was estimated using Eq. 9 for selected experiments among those reported in Figure 5; the results are summarized in Table 1. The emissivity of K_2CO_3 was taken as $\epsilon = 1.0$ (black-body assumption); the thermal conductivity of water vapor within the range 313 to 353 K is approximately $\lambda_v = 0.02$ W/m·K. Except for the more rapid dehydrations of particles larger than 125 to 149 μm (−100 + 120 mesh), the magnitude of the maximum self-cooling effect was estimated to be less than 1 K. With increasing particle size, the increase in self-cooling should result in a decrease in reaction rate and may be responsible for the slightly skewed bias of the data points in Figures 3 and 4 as compared with the straight-line prediction. In fact, this bias seems to diminish for slower dehydrations, as expected if the self-cooling effect diminishes.

Also of interest are the relative contributions to heat transfer from conduction and radiation, as estimated by the two terms in the LHS of Eq. 9. For the 590 to 710 μm (−25 +30 mesh) particles, radiation accounted for about 14% of the total heat transferred, independent of the reaction rate; while for the 125 to 149 μm (−100 +120 mesh) particles, the figure was only about 3%. Thus conduction from the vapor to the particle appears to be the primary mode of external heat transfer.

In a vacuum, however, radiation is the only mode of heat transfer. Since Eq. 6 showed that there is only negligible resistance to heat transfer in the product layer, and since the particles share a finite contact area with the sample pan because they are in reality irregular and not spherical, the resistance to conduction from the pan to the dehydration interface may be considered small. If the particle and pan temperatures are assumed to be identical, the dynamic temperature behavior of the system consisting of the pan and particles is described by the heat balance equation:

$$(m_1C_{p1} + m_2C_{p2})\frac{dT_p}{dt} = (5.67 \times 10^{-8})(A_1\epsilon_1 + A_2\epsilon_2)(T_b^4 - T_p^4) - m_1\Delta H_1\frac{dX}{dt} \quad (10)$$

where m_1 and m_2 are the weights, C_{p1} and C_{p2} are the specific heats, and A_1 and A_2 are the areas of the hydrate sample and aluminum sample pan, respectively. The rate of dehydration as a function of time is given by:

$$\frac{dX}{dt} = 3\,(-\dot{r}/r_o)\,[1 - (-\dot{r}/r_o)t]^2 \quad (11)$$

The nonlinear temperature term in Eq. 10 may be linearized for small values of $(T_b - T_p)$ using the expression:

$$(T_b^4 - T_p^4) \cong 4T_b^3(T_b - T_p) \quad (12)$$

Defining the deviation variable $\overline{T}_p = (T_b - T_p)$, the solution to Eq. 10 using Eqs. 11 and 12 yields the temperature change of the particles-and-pan system as a function of time:

$$\overline{T}_p = \Omega\{[1 + 2\tau(-\dot{r}/r_o) + 2\tau^2(-\dot{r}/r_o)^2][1 - \exp(-t/\tau)] - 2[(-\dot{r}/r_o) + \tau(-\dot{r}/r_o)^2]\,t + (-\dot{r}/r_o)^2t^2\} \quad (13)$$

where

Table 2. Estimated Maximum Degrees of Self-Cooling for Vacuum Dehydration of $K_2CO_3 \cdot 3/2H_2O$ Particles from 125 to 149 μm (−100 + 120 Mesh)

Furnace Temp. K	Calc. Max. Self-Cooling, K
357.7	12.4
351.7	6.2
345.7	5.2
340.7	4.3
336.7	3.5
333.7	3.2
328.7	2.6
323.7	2.0
320.7	1.3

$$\Omega = \frac{3m_1\Delta H_1(-\dot{r}/r_o)}{4(5.67 \times 10^{-8})T_b^3(A_1\epsilon_1 + A_2\epsilon_2)} \quad (14)$$

and

$$\tau = \frac{m_1C_{p1} + m_2C_{p2}}{4(5.67 \times 10^{-8})T_b^3(A_1\epsilon_1 + A_2\epsilon_2)} \quad (15)$$

The sample pan weighed m_2 = 81 mg and had an estimated area $A_2 = 4$ cm^2, the emissivity of oxidized aluminum is approximately $\epsilon_2 = 0.15$ (Weast, 1977), the heat capacities of both K_2CO_3 and aluminum near 350 K are approximately $C_{p1} \cong C_{p2} \cong 920$ J/kg-K; values for m_1, ΔH_1, T_b, and $(-\dot{r}/r_o)$ were obtained from the experimental results.

The maximum degrees of self-cooling were calculated using Eq. 13 for each furnace temperature studied (Table 2). Using these results as a correction to the furnace temperature to obtain a more accurate particle temperature, each calculated interface velocity is plotted against the revised temperature on Arrhenius coordinates in Figure 6. The corrected data fall along a straight line that is given by a least-squares fit as:

$$\ln(-\dot{r}) = (-10{,}900/T) + 21.3 \quad (16)$$

The slope of this line is 10,900 ± 500 K and the intercept is 21.3 ± 0.1 when $-\dot{r}$ is expressed in cm/s.

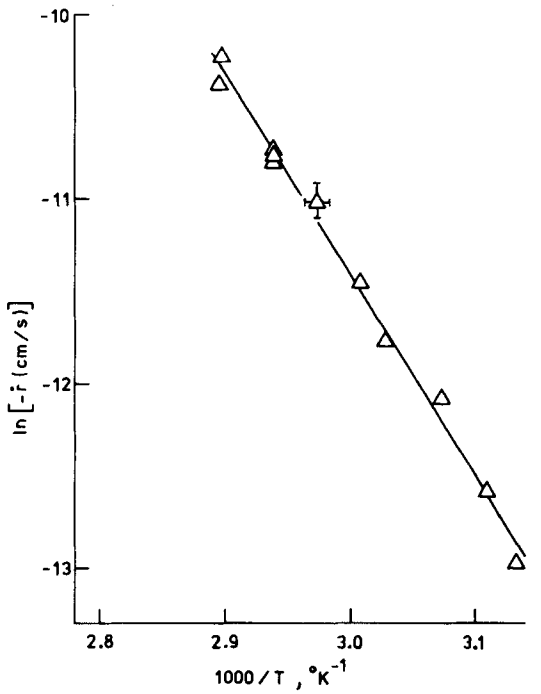

Figure 6. Vacuum dehydration rates of $K_2CO_3 \cdot 3/2H_2O$ crystals on Arrhenius coordinates, corrected for the effects of self-cooling.

Diffusional Effects

An atmosphere of pure water vapor effectively eliminates the mass transfer resistances associated with an external boundary layer and with binary pore-diffusion that are often encountered in gas-solid reactions. However, Knudsen diffusion of water vapor through the solid may be important in these experiments, since the mean free paths of the vapor molecules (no less than 5μm for the ranges of pressures and temperatures studied) were considerably larger than the pore of the solid (less than 1 μm). For a porous solid the effective diffusivity is (Satterfield, 1980):

$$D = (\omega/\tau_s)\, 97.0\, r_e (T/M)^{1/2} \tag{17}$$

where ω is the void fraction and τ_s is the tortuosity factor of the solid. The mean pore radius, r_e, may be defined empirically as

$$r_e \equiv \frac{\int_{V_1}^{V_2} r\, dV}{(V_2 - V_1)} \tag{18}$$

where dV is the volume of pores having radii between r and $r + dr$.

For a spherical particle undergoing shrinking-core dehydration, the equation governing diffusion of water through the product layer is:

$$D\left[\frac{1}{r^2}\frac{\partial}{\partial r}\left(r^2\frac{\partial c}{\partial r}\right)\right] = 0 \tag{19}$$

with the boundary conditions

$$D\frac{\partial c}{\partial r} = (\rho/0.018)\dot{r} \tag{20}$$

at the surface of the unreacted core ($r = r_s$), and

$$c = c_b \tag{21}$$

at the external surface of the particle ($r = r_o$). Assuming that the water vapor behaves as an ideal gas at the low pressures studied, (P/RT) may be substituted for c. The solution to these equations gives the pressure in the product layer as a function of radius

$$P = P_b + (\rho R T r_s \dot{r}/0.018D)(r_s/r_o - r_s/r) \tag{22}$$

from which one obtains the pressure difference across the product layer.

$$(P_s - P_b) = [\rho R T r_o \bar{r}(1 - \bar{r})/0.018D]\,(-\dot{r}) \tag{23}$$

where P_s is the pressure at the core surface and P_b is the external pressure imposed.

The significance of the diffusional resistance of the product layer may be estimated from experimental dehydration rate and porosimetry data using Eqs. 17 and 23. According to Eq. 17, the effective diffusivity of water vapor in the product layer depends on the void fraction, tortuosity, and effective mean pore radius of the solid. The results of porosimetry measurements on the solid particles produced by the dehydration of $K_2CO_3 \cdot 3/2H_2O$ at 353 K under 1.5 kPa water vapor are shown in Figure 7. They yield a mean pore raidus $r_e = 0.11$ μm from Eq. 18 and a void fraction $\omega = 0.15$ in pores greater than 100 Å in diameter. The tortuosity factor cannot be evaluated directly; however, the tortuosities of commercial catalysts with void fractions of about 0.7 to 0.3 are known to vary in the range from about 2 to 7 (Satterfield, 1980). Since the void fraction of the dehydration product calculated from porosimetry was only about 0.15, the tortuosity factor is probably near the high end of the known range and is thus assumed here to be $\tau_s = 7$. With the parameters given above, Eq. 17 predicts that at 353 K, the effective Knudsen diffusivity of water vapor in the product layer is $D = 1.0 \times 10^{-6}$ m^2/s.

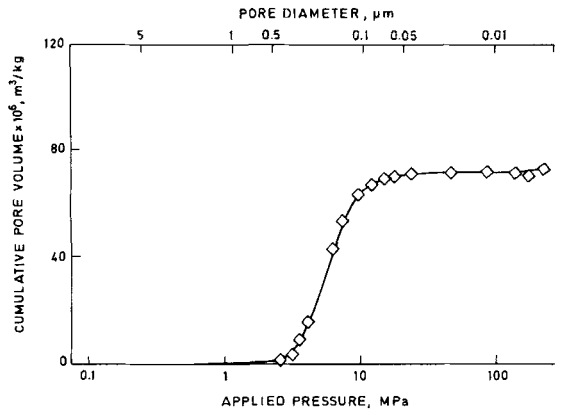

Figure 7. Pore volume data for K_2CO_3 particles prepared from 300 to 354 μm (−45 + 50 mesh) $K_2CO_3 \cdot 3/2H_2O$ crystals at T = 353 K and P = 1.5 kPa.

TABLE 3. ESTIMATED MAXIMUM PRESSURE DROP ACROSS PRODUCT LAYER FOR DEHYDRATION OF $K_2CO_3 \cdot 3/2H_2O$ PARTICLES IN WATER VAPOR

Temp. K	Pres. Pa	Calc. Interface Velocity, μm/min	Calc. Pres. Drop, Pa: 590 to 710μm (−25 + 30 Mesh)	Calc. Pres. Drop, Pa: 125 to 149μm (−100 + 120 Mesh)
358	270	17	1,300	270
358	610	12.3	930	200
358	1,300	5.4	410	87
358	1,850	0.86	67	15
348	270	7.8	570	120
348	750	1.7	130	27
338	270	1.7	120	27

Using this diffusivity, the maximum pressure difference (occurring at $\bar{r} = 0.5$) across the product layer was estimated using Eq. 23 for the same dehydration experiments for which thermal effects were listed in Table 1. The results, Table 3, could be interpreted to support the argument that diffusional resistance is significant for rapid dehydrations of large 590 to 710 μm (−25 + 30 mesh) particles, but virtually negligible for slow dehydrations of small 125 to 149 μm (−100 + 120 mesh) particles. However, such a fine distinction is questionable in view of the empiricism and uncertainty associated with the calculation of the effective Knudsen diffusivity from Eq. 17. In fact, errors in the estimation of tortuosity, mean pore radius, and void fraction could realistically account for an order-of-magnitude uncertainty in the diffusivity. Therefore, other means of evaluating diffusional effects are needed. Experimental evidence does appear to indicate that mass-transfer limitations are negligible. According to Eq. 23, the difference between the pressure at the dehydration interface and that at the external surface of the particle varies as $\bar{r}(1 - \bar{r})$; thus it is negligible at the beginning and end of the reaction but rises to a maximum at $\bar{r} = 0.5$ ($X = 0.875$). Since the interface velocity has been shown to be very sensitive to pressure (Figure 5), it would be expected in the absence of thermal effects to decrease with conversion to X = 0.875 and then rise again for the remainder of the reaction. Also, since the pressure at the interface depends on $(-r)$ according to Eq. 23, the variation of interface velocity with conversion should be most pronounced during the most rapid dehydrations.

If the estimates in Table 3 are accurate, the data from experiments with 590 to 710 μm (−25 + 30 mesh) particles would be expected to deviate significantly from the predictions of Eq. 1 since the pressure at the dehydration interface is expected to vary several hundred Pa during the reaction. Figure 8 shows no trace of these deviations, suggesting that the diffusional resistances characterized by the estimates in Table 3 have been overestimate and that in reality, the rate of mass transfer does not significantly limit the overall reaction rate in these experiments.

Although the numerical estimates in Table 3 must be considered ambiguous in view of their margin of uncertainty, they are probably in error by no more than one order of magnitude. Thus, the conclusions are that mass transfer resistance was not significant in these measurements, but that the experimental conditions employed and the rates encountered were probably near the threshold at which diffusion begins to be important.

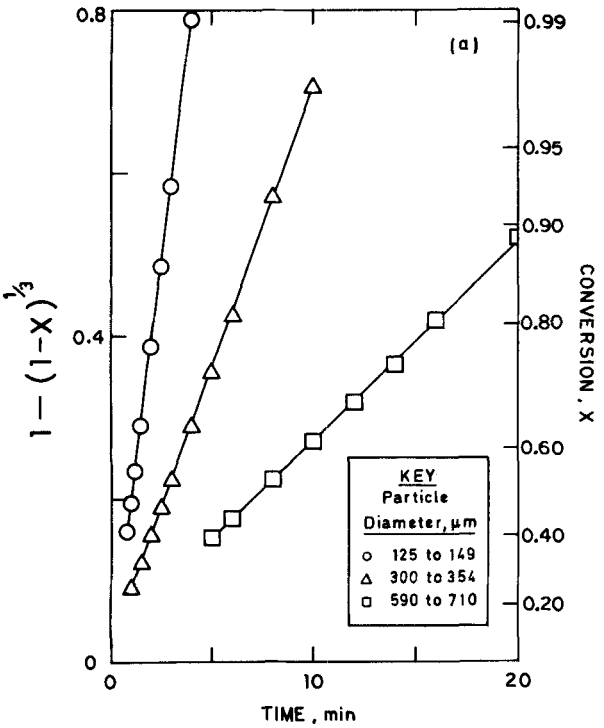

Figure 8. Dehydration data for $K_2CO_3 \cdot 3/2H_2O$ crystals at $T = 358$ K, $P = 610$ Pa.

ACKNOWLEDGMENT

This research was supported by the U.S. Department of Energy through the Solar Energy Research Institute under Contract No. DE-FG02-80CS-84051-A002.

NOTATION

A = area, m^2
C_p = specific heat, J/kg·K
c = concentration, mol/m^3
D = effective Knudsen diffusivity for a porous solid, m^2/s
G = integrated rate expression, dimensionless
ΔH = enthalpy of decomposition per unit mass of product, J/kg
ΔH_1 = enthalpy of decomposition per unit mass of hydrate, J/kg
M = molecular weight, kg/kmol
m = mass, kg
P = pressure, Pa
Q = rate of heat transfer, W
R = gas constant, J/mol·K
r = radius, m
$\dot{r}$ = interface velocity, m/s
$\bar{r}$ = dimensionless radius
r_o = initial particle radius, m
T = temperature, K
t = time, s
V = volume, m^3
X = conversion, dimensionless

Greek Letters

ϵ = emissivity, dimensionless
λ = thermal conductivity of product layer, W/m·K
λ_v = thermal conductivity of vapor, W/m·K
ρ = density of water in hydrate crystal, kg H_2O/m^3
τ = time constant defined by Eq. 15
τ_s = tortuosity factor, dimensionless
Ω = coefficient defined by Eq. 14
ω = void fraction, dimensionless

Subscripts

1 = hydrate
2 = aluminum sample pan
b = bulk
c = conduction
e = effective
eq = equilibrium
p = particle
r = radiation
s = surface of unreacted core
v = vapor

LITERATURE CITED

Acock, G. P., W. E. Garner, J. Milsted, and H. J. Willavoys, "The Dehydration of Ammonium, Potassium, and Some Mixed Alums," *Proc. R. Soc.*, **189**, 508 (1946).

Anous, M. M. T., R. S. Bradley, and J. Colvin, "The Rate of Dehydration of Chrome Alum," *J. Chem. Soc.*, 3348 (1951).

Baughn, J., and Alan Jackman, "Solar Energy Storage Within the Absorption Cycle," ASME Paper 74-WA/HT-18, ASME Winter Annual Meeting, New York (Nov. 17–22, 1974).

Cooper, M. M., J. Colvin, and J. Hume, "The Dehydration of Copper Sulphate Trihydrate," *Trans. Farad. Soc.*, **29**, 576 (1933).

Cooper, J. A., and W. E. Garner, "The Dehydration of Crystals of Chrome Alum," *Proc. R. Soc.*, **A174**, 487 (1940).

Fichte, P. M., and T. B. Flanagan, "Kinetics of Dehydration of Single Crystals of Copper Formate Tetrahydrate," *Trans. Farad. Soc.*, **67**, 1467 (1971).

Gardet, J. J., "The Dehydration Kinetics of Calcium Sulphate Dihydrate. Influence of the Gaseous Atmosphere and the Temperature," *Cem. Concr. Res.*, **6**, 697 (1976).

Ishida, M., M., Kamata, and T. Shirai, "Kinetic Studies of Thermal Dehydration of Gypsum and Application of Reaction Diagram," *J. Chem. Eng. Japan*, 3(2), 201 (1970).

Ishida, M., and T. Shirai, "Graphical Representation of Solid-Gas Reactions Based on Unreacted Core Model," *J. Chem. Eng. Japan*, **2**(2), 175 (1969).

Ishida, M. and T. Shirai, "Reaction Diagram for Reversible Solid-Gas Reactions Based on Unreacted Core Model," *J. Chem. Eng. Japan*, **3**(2), 196 (1970).

Ishida, M., and C. Y. Wen, "Comparison of Kinetic and Diffusional Models for Solid-Gas Reactions," *AIChE J.*, **14**(2), 311 (1968).

Lyakhov, N. Z., and V. V. Boldyrev, "Kinetics and Mechanism of the Dehydration of Crystal Hydrates," *Russ. Chem. Rev.*, **41**(11), 919 (1972).

McAdie, H. G., "The Effect of Water Vapor Upon the Dehydration of $CaSO_4 \cdot 2H_2O$," *Can. J. Chem.*, **42**, 792 (1964).

Satterfield, C. N., *Heterogeneous Catalysis*, McGraw-Hill, New York (1980).

Sharp, J. H., G. W. Brindley, and B. N. Narahari Achar, "Numerical Data for Some Commonly Used Solid State Reaction Equations," *J. Amer. Cer. Soc.*, **49**(7), 379 (1966).

Shen, J., and J. M. Smith, "Diffusional Effects in Gas-Solid reactions," *Ind. Eng. Chem. Fund.*, **4**(3), 293 (1965).

Smith, M. L., and B. Topley, "The Experimental Study of the Rate of Dissociation of Salt Hydrates. The Reaction $CuSO_4 \cdot 5H_2O \rightleftarrows CuSO_4 \cdot H_2O + 4H_2O$," *Proc. R. Soc.*, **A134**, 224 (1931).

Stanish, M. A., and D. D. Perlmutter, "Salt Hydrates as Absorbents in Heat Pump Cycles," *Solar Energy*, **26**(4), 333 (1981).

Szekely, J., and J. W. Evans, "A Structural Model for Gas-Solid Reactions With a Moving Boundary," *Chem. Eng. Sci.*, **25**, 1091 (1970).

Szekely, J., and J. W. Evans, "A Structural Model for Gas-Solid Reactions With a Moving Boundary: II. The effect of grain size, porosity, and temperature on the reaction of porous pellets," *Chem. Eng. Sci.*, **26**, 1901 (1971).

Weast, R. C., Ed., *CRC Handbook of Chemistry and Physics*, CRC Press, West Palm Beach (1977).

Wen, C. Y., "Noncatalytic Heterogeneous Solid Fluid Reaction Models," *Ind. Eng. Chem.*, **60**(9), 34 (1968).

Wen, C. Y., and S. C. Wang, "Thermal and Diffusional Effects in Noncatalytic Solids Gas Reactions," *Ind. Eng. Chem.*, **62**(8), 30 (1970).

Manuscript received March 11, 1982; revision received October 18, and accepted October 28, 1982.